J. Phys. D: Appl. Phys. **42** (2009) 145412 (5pp) doi:10.1088/0022-3727/42/14/145412

A single-gap transflective liquid crystal driven by fringe and vertical electric fields

Young Jin Lim[1], Mi Hyung Chin[1], Jin Ho Kim[1], Jung Hwa Her[1], Hyun Suk Jin[2], Byeong Koo Kim[2] and Seung Hee Lee[1]

[1] Polymer BIN Fusion Research Center, Department of Polymer Nano-Science and Technology, Chonbuk National University, Chonju, Chonbuk 561-756, Korea
[2] Mobile Product Development Department, LG Display Co., Ltd., Gumi, Gyungbuk 730-350, Korea

E-mail: lsh1@chonbuk.ac.kr (SHL)

Received 23 April 2009, in final form 8 June 2009
Published 3 July 2009
Online at stacks.iop.org/JPhysD/42/145412

Abstract
A single-gap transflective liquid-crystal display driven by a fringe electric field in the transmissive (T) region and a vertical electric field in the reflective (R) region was designed. In the device, a homogeneously aligned liquid crystal (LC) rotates almost in plane by a fringe field in the T-region whereas the LC tilts upwards by a vertical field in the R-region. A high surface pre-tilt angle of the LC in the R-region is achieved through polymerization of an UV curable reactive mesogen monomer at the surfaces and thus the effective cell retardation in the R-region becomes half of that in the T-region. Consequently, a transflective display driven by a vertical and a fringe electric field with a single cell gap and single gamma curves is realized.

(Some figures in this article are in colour only in the electronic version)

1. Introduction

Recently, transflective liquid-crystal displays (LCDs) have been actively investigated for portable devices such as mobile phones, personal digital assistants (PDAs) and digital cameras because they show good visibility in any environmental lighting conditions. However, initial transflective LCDs required a dual cell gap structure with several compensation films so that the devices matched the optical path of the R- and T-regions [1, 2]. To solve these problems, single cell gap transflective LCDs have been proposed using several liquid crystal (LC) modes, such as vertical alignment (VA) [3, 4], and fringe-field switching (FFS) [5–10] and in-plane switching (IPS) [11–14] with homogeneous alignment and twisted nematic (TN) [15, 16]. Among these, the IPS and FFS modes show a wide viewing angle and the FFS mode has a high light efficiency using an in-cell retarder with a quarter-wave plate. However, these devices show wavelength dispersion in the R-region because the dark state makes two passes through the patterned in-cell retarder with the quarter-wave plate. In order to solve this problem, several researchers proposed transflective LCD driven by FFS in the T-region and electrically controlled birefringence (ECB) using a patterned in-cell retarder with a half-wave plate [17–19] in the R-region. However, these devices still need to be improved because the cell gaps of the T- and R-regions are different, the gamma curves between the voltage-dependent R_R and T_T curves do not match well and the optical light efficiency is still not satisfactory.

In this paper, we propose a single-gap transflective LCD driven by a fringe electric field in the T-region and a vertical electric field in the R-region. To achieve a single cell gap display, a high surface pre-tilt angle in the R-region is formed through polymerization of an UV curable reactive mesogen (RM) monomer at the surface when the voltage is applied. With further optimization of the cell structure the device can have a single gamma curve.

2. Switching principle and cell condition

Figure 1 shows the cross-sectional and top view of the proposed single cell gap transflective LCD driven by fringe and vertical electric fields. In the device, both pixel and common electrodes exist on the bottom substrate with a passivation layer between them in the T-region. In the R-region, the pixel electrode exists on the bottom substrate but the common electrode exists on the top substrate. The pixel electrode of the T-region is patterned with an electrode width (w) and distance (l) between them and the pixel electrode in the R-region is non-patterned. On the top substrate, the in-cell retarder is patterned to have a

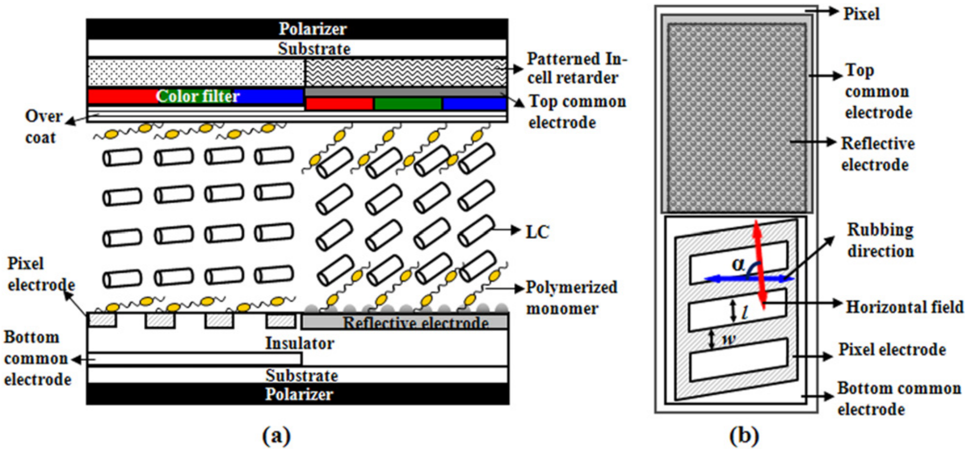

Figure 1. Electrode structure of the transflective display driven by fringe and vertical electric fields: (*a*) cross-sectional and (*b*) top view.

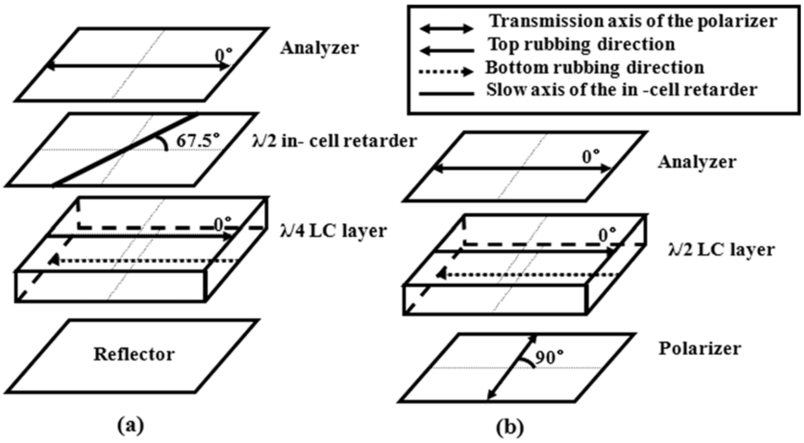

Figure 2. Optical configurations of the optical layers in the device: (*a*) R- and (*b*) T-regions.

retardation of $\lambda/2$ only in the R-region using a metal mask and UV [20]. The common electrode of the R-region is formed below the patterned in-cell retarder, and then the colour filter is formed. Here, the thickness of the in-cell retarder is 2 μm. The rubbing direction is parallel to the analyzer in both the T- and the R-regions and the polarizer axis is orthogonal to the analyzer.

In the device where uniaxial LC medium exists under crossed polarizers, the transmittance (T_{T}) is given by

$$T_{\mathrm{T}} = T_{\mathrm{o}} \sin^2 2\psi(V) \sin^2(\delta/2),$$

where ψ is the angle between the polarizer and the LC director and δ is the phase difference between the ordinary and the extraordinary rays, defined by $\delta = 2\pi d \Delta n_{\mathrm{eff}}(V)/\lambda$, where d is the cell gap and Δn_{eff} is the voltage-dependent effective birefringence of the LC layer and λ is the incident wavelength.

The optical configuration of the proposed single-gap transflective LCD is shown in figure 2. In the initial state, the analyzer axis and the optic axis of the LC layer coincide with each other and the optic axis of the in-cell retarder with $\lambda/2$ retardation in the R-region makes 67.5° with respect to the analyzer. To obtain a dark state in the R-region, the retardation of the LC layer should be $\lambda/4$. In the T-region, the optimal cell $d\Delta n$ of the LC layer for achieving effective

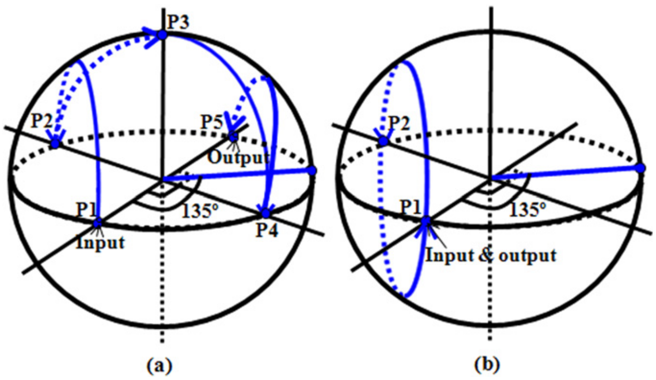

Figure 3. Poincaré sphere representation of the polarization path of the (*a*) dark and (*b*) white states in the R-region and the (*c*) dark and (*d*) white states in the T-region.

$\lambda/2$ is 0.40 μm [21]. Therefore, in order for the $d\Delta n$ of the LC layer to be $\lambda/4$ in the R-region, a high surface tilt angle is required. According to our calculation and also experiment, the pre-tilt angles of the R-region should be 53°.

Figure 3 shows the polarization state in the R-region on a Poincaré sphere. In the absence of voltage, the linearly polarized light (P1) passing through the top polarizer changes the polarization direction to 135° after passing through the in-cell retarder since the angle between the polarizer and the

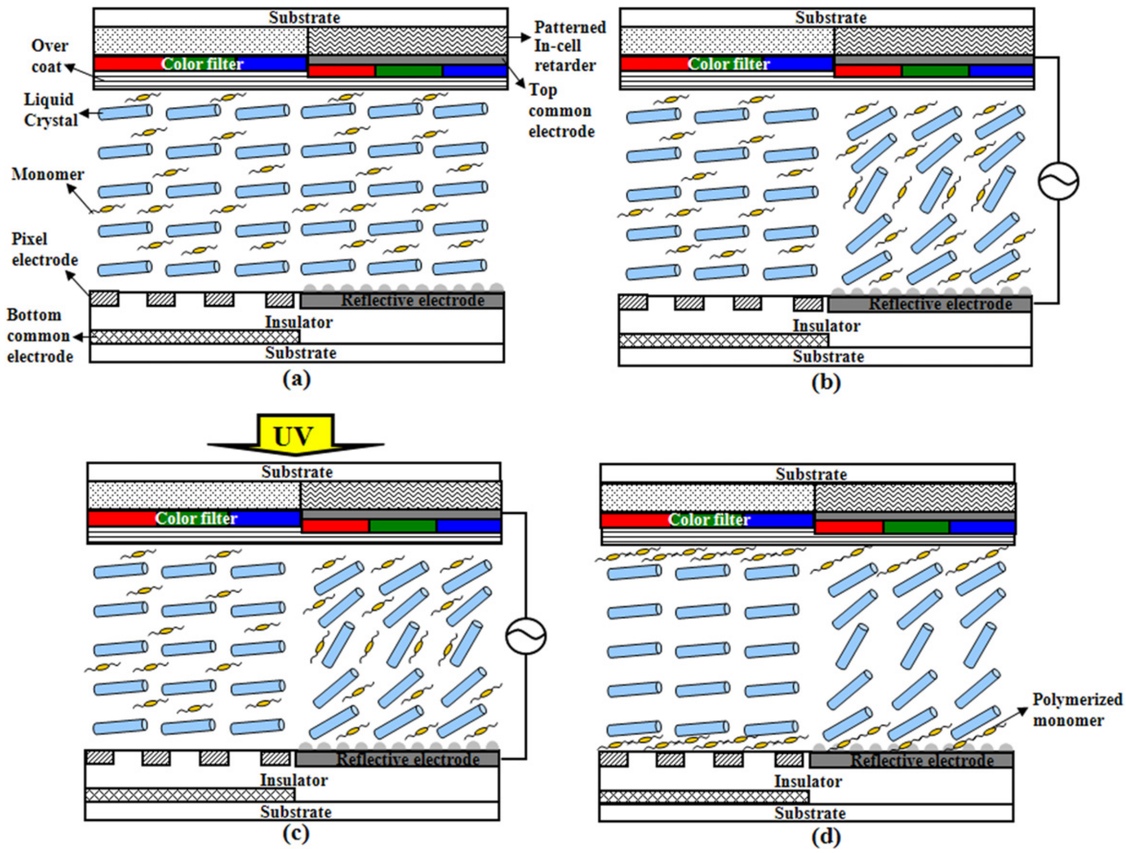

Figure 4. Schematic diagram of the processes for fabricating the proposed transflective LCD with defined pre-tilt angles at the substrate surfaces in the R-region.

in-cell retarder is 67.5°. Next, the linearly polarized light (P2) becomes circularly polarized (P3) after passing through the LC. The reflected light by the reflector becomes linearly polarized (P4) with a polarization direction of 45° after passing through the LC, again. Finally, it becomes linearly polarized (P5) with a polarization direction of 90° after passing through the in-cell retarder again, and then it is blocked by the analyzer as shown in the Poincaré sphere of figure 3(*a*). With the bias voltage, the LC director of the R-region tilts up in the vertical directions in response to the vertical electric field, and thus its phase retardation becomes zero. So, the linearly polarized light (P1) changes direction only by 135° and the linearly polarized light propagates the LC layer without changing the polarization state (P2). The reflected light passes through the LC cell and the in-cell retarder again and then the vibration direction of the linearly polarized light is the same as the original (P1), resulting in a bright state, as described in figure 3(*b*).

According to the switching principle described above, the reflectance (R_R) in the R-region is given by $R_R = R_o \sin^2(\delta)$ such that it is maximal at $\delta = \pi/2$ and minimal at $\delta = 0$. In other words, it is determined by only the phase difference in the R-region.

3. Results and discussion

For electro-optic calculations, a commercially available LCD simulator (Shintech, Japan) was used. In the T-region, the width of the pixel electrode is 3 μm and its distance between the electrodes is 4.5 μm and the pixel electrode structure of the R-region is a patterned plane form. The cell gap of both the T- and R-regions is 4 μm. Here, the nematic LC with physical parameters such as dielectric anisotropy $\Delta\varepsilon = 7.4$, elastic constants $K_1 = 11.7$ pN, $K_2 = 5.1$ pN, $K_3 = 16.1$ pN and birefringence $\Delta n = 0.1$ are used, and the surface tilt angle of the LC is 2° and 53° in the T- and R-regions, respectively. Here, to calculate the R_R and T_T, a 2×2 extended Jones matrix was used [22]. The transmittances for the single polarizer and the parallel polarizers are assumed to be 41% and 35%, respectively.

Next, the manufacturing process for achieving a high surface pre-tilt angle of the LC in the R-region through polymerization of an UV curable RM at the surfaces is explained. For the experiment, the super-fluorinated nematic LC mixture (from Merck-Korea) is used and its physical parameters are the same as those in the simulation condition. The LC mixture is mixed with RM-257 (from Merck) and a photo-initiator, Irgacure 651 (from Ciba). Two different weight percentages of the monomer relative to the LC, 0.1% and 0.5%, are evaluated. The weight percentage of the photo-initiator relative to the LC is 0.01%. Then, the mixture is heated to the isotropic temperature of the LC for 5 min to obtain a homogeneous mixture.

Figure 4 shows the schematic diagram of the processes for fabricating the proposed transflective LCD with defined pre-tilt angles at the substrate surfaces in the R-region. Initially,

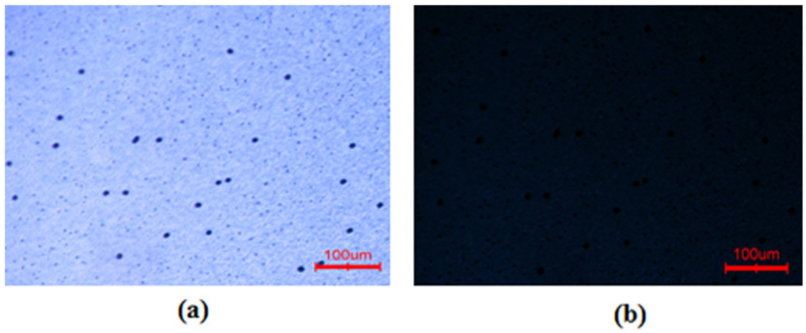

Figure 5. Polarization microphotographs of (*a*) off and (*b*) on states of the fabricated test cell with weight per cent of RM equal to 0.5%. The dark spots in the off state come from the existence of bar spacers.

the RM monomer is also aligned homogeneously along the LC layer due to the use of homogeneous alignment layers on both substrates, as shown in figure 4(*a*). Then, a voltage higher than the threshold voltage is applied to the R-region so that the RM monomer and the LC could be reoriented with some tilt angle from the surface in response to the vertical electric field [23, 24], as shown in figure 4(*b*). In the presence of an electric field, the cell is exposed to UV light and thus the monomers are polymerized with a constant tilt angle at the surfaces through a photo-induced monomer diffusion process under optimal monomer weight per cent and UV curing condition, as shown in figure 4(*c*). Consequently, in the absence of an electric field, the LCs in the bulk relax to the original homogeneous state while the surfaces have some defined pre-tilt angles at 2° and 53° in the T- and R-regions, respectively, as shown in figure 4(*d*).

To prove the uniform pre-tilt angle of the LC, the fabricated test cell with a weight per cent of RM equal to 0.5% was observed under crossed polarizer polarization microscopy (Nikon DXM1200) in which the cell was located with its optic axis making an angle of 45° with respect to the crossed polarizer. Figure 5 shows polarization microphotographs before and after applying voltage. In the off state, no defects related to the RM monomer were observed. As a result, a uniform transmittance was generated, as shown in figure 5(*a*). In the on state with 10 V, we observed a uniform dark state without a declination line. This indicates that the vertical electric field tilts up the LC molecules with a high tilt angle to the field direction in the whole region, as shown in figure 5(*b*).

Figure 6 shows the measured retardation as functions of applied voltage for two different concentrations of the RM monomer. The effective cell retardation at 0 V is 400 nm; however, with polymerization of the RM monomer when the voltage is applied, it is reduced due to the generation of a surface tilt angle by the polymerized RM. One interesting factor is that the decreasing rate of retardation is relatively small when the weight per cent of RM is 0.1%, that is it decreases to 380 nm when 10 V is applied. However, with an increase in weight per cent of RM to 0.5%, the cell retardation decreases from 400 nm (0 V) to 140 nm (10 V). Consequently, through optimization of the concentration of the RM monomer into the LC mixture and UV dosage condition with proper bias voltage, a high surface tilt angle which has a $d\Delta n_{\mathrm{eff}}$ of $\lambda/4$

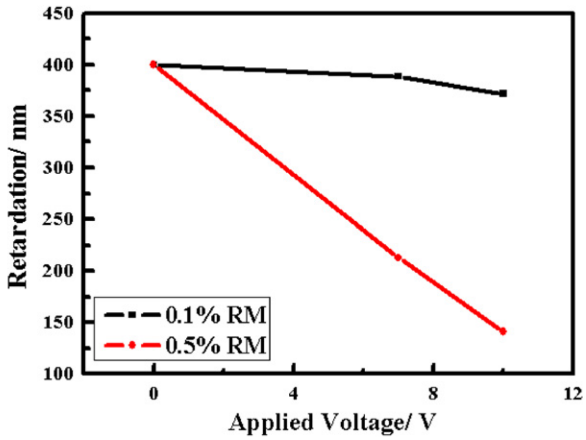

Figure 6. Measured retardation as variations of applied voltage for two different concentrations of the RM monomer.

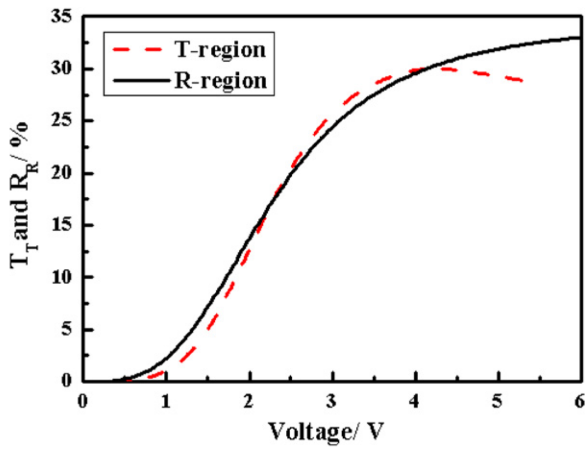

Figure 7. Voltage-dependent reflectance and transmittance curves.

in the R-region is achieved. Through utilization of the RM monomer, we could achieve singe cell gap transflective display.

Now, another issue for the proposed transflective display is whether the device shows a single gamma curve. Figure 7 shows voltage-dependent R_{R} and T_{T} curves. Here, the angle α between the horizontal component of the fringe electric field and the LC director is 80°. As indicated, both curves do not match perfectly. The operating voltage (V_{op}) in the T-region is 4.2 V; however, R_{R} increases with increasing voltage in the

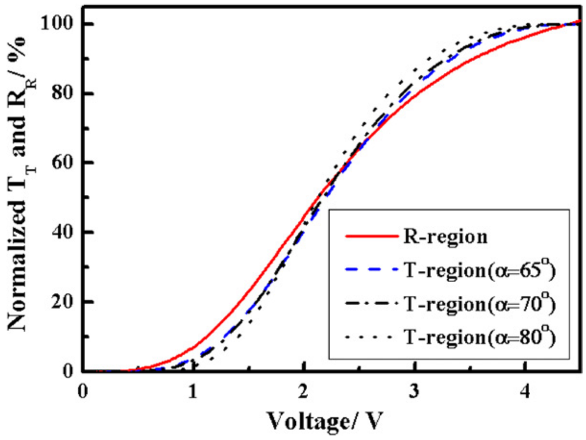

Figure 8. Voltage-dependent normalized transmittance curves as a function of different αs with voltage-dependent reflectance curve.

R-region because it can be maximal when the cell retardation becomes zero, which is not possible due to strong anchoring energy between the polymer and the LC molecules. Therefore, in order to match both curves, we reduced the V_{op} of the R-region to match the V_{op} of the T-region, resulting in a small sacrifice in the reflectance. However, R_R is 30% at that voltage and still its optical efficiency is about 87%. In the FFS device, the voltage-dependent T_T curve is dependent on α [25]. In order to find closer matching conditions between both curves, we calculated the voltage-dependent T_T curves as a function of αs , as shown in figure 8. In the T-region, as α decreases from 80° to 65°, V_{op} increases while the threshold voltage decreases, so both the voltage-dependent T_T and R_R curves match slightly better when α is 65°.

4. Summary

In summary, a single-gap transflective display with dual mode, in which the R-region is with the ECB mode and the T-region is with the FFS mode, is proposed. To make a single cell gap, a high pre-tilt angle is formed in the R-region through polymerization of an UV curable RM monomer at the surface of the alignment layers. In addition, the device can be driven by single gamma curves. This new device has the potential to become an integral part of transflective displays.

Acknowledgments

This work was supported by the Korea Research Foundation Grant funded by the Korean Government (MOEHRD, Basic Research Promotion Fund) (KRF-2007-511-D00071) and in part by LG Displays.

References

[1] Shibazaki M, Ukawa Y, Takahashi S, Iefuji Y and Nakagawa T 2003 *Soc. Inform. Disp. Tech. Dig.* **34** 90
[2] Fukuda I, Sakurai Y, Nakata T and Sakamoto Y 2005 *Proc. 12th Int. Display Workshops (Takamatsu, Japan)* p 107
[3] Kang S G, Kim S H, Song S C, Park W S, Yi C, Kim C W and Chung K H 2004 *Soc. Inform. Disp. Tech. Dig.* **35** 31
[4] Lo Ch, Yang T-Ch, Hu Ch-J, Cheng Ch-Sh, Chang Ch-M and Gan F-Y 2007 *Soc. Inform. Disp. Tech. Dig.* **38** 714
[5] Lim Y J, Song J H, Kim Y B and Lee S H 2004 *Japan. J. Appl. Phys.* **43** L972
[6] Choi M O, Song J H, Lim Y J and Lee S H 2005 *Soc. Inform. Disp. Tech. Dig.* **36** 719
[7] Song J H, Lim Y J, Lee M-H, Lee S H and Shin S T 2005 *Appl. Phys. Lett.* **87** 011108
[8] Lim Y J, Lee M-H, Lee G-D, Jang W-G and Lee S H 2007 *J. Phys. D: Appl. Phys.* **40** 2759
[9] Kim H Y, Ge Z, Wu S-T and Lee S H 2007 *Appl. Phys. Lett.* **91** 231108
[10] Ge Z, Wu S-T and Lee S H 2008 *Opt. Lett.* **33** 2623
[11] Yu I H, Song J H, Lim Y J, Lee S H, Kim D S, Soh H-S, Kim W Y and Yeo S D 2004 *Proc. 11th Int. Display Workshops (Niigata, Japan)* p 167
[12] Song J H and Lee S H 2004 *Japan. J. Appl. Phys.* **43** L1130
[13] Song J H, Lee S H, Kim D S, Soh H-S and Kim W Y 2005 *Mol. Cryst. Liq. Cryst.* **433** 105
[14] Park K H, Ko Y J, Kim J C and Yoon T H 2004 *Proc. 11th Int. Display Workshops (Niigata, Japan)* p 163
[15] Ge Z, Zhu X and Wu S-T 2006 *J. Disp. Technol.* **2** 102
[16] Mak M-Y, Xu P, Li X, Chigrinov V G and Kwok H-S 2007 *Japan J. Appl. Phys.* **46** 7798
[17] Imayama H, Tanno J, Igeta K, Morimoto M, Itou O and Hirota S 2007 *Soc. Inform. Disp. Tech. Dig.* **38** 1651
[18] Hirota S, Oka S, Itou O, Igeta K, Morimoto M, Imayama H, Komura S and Nagata T 2007 *Soc. Inform. Disp. Tech. Dig.* **38** 1661
[19] Koma N, Mitsui M, Tanaka Y and Endo K 2007 *Soc. Inform. Disp. Tech. Dig.* **38** 1270
[20] Kim J, Lim Y-W and Lee S-D 2006 *Japan. J. Appl. Phys.* **45** 810
[21] Jung S H, Kim H Y, Song S H, Kim J-H, Nam S-H and Lee S H 2004 *Japan. J. Appl. Phys.* **43** 1028
[22] Lien A 1990 *Appl. Phys. Lett.* **57** 2767
[23] Chen T J and Chu K-L 2008 *Appl. Phys. Lett.* **92** 091102
[24] Lim Y J, Jeong E, Chin M H, Kim J H, Kim S S and Lee S H 2008 *Proc. Spring Symp. of the Korean Institute of Electrical and Electronic Material Engineers (Asan, Chungnam, Korea)* p 51
[25] Hong S H, Park I C, Kim H Y and Lee S H 2000 *Japan. J. Appl. Phys.* **39** L527